PACS numbers: 42.55.Vc; 42.60.Lh
DOI: 10.1070/QE2008v038n10ABEH013686

X-ray laser on transitions of Pd-like ions from ErXXIII to ReXXX

E.P. Ivanova

Abstract. **The wavelengths, the rates of processes, and the gains of spontaneous emission at the transitions of Pd-like ions from ErXXIII to ReXXX are calculated for the first time. The high quantum yield of amplified emission in these ions is possible at transitions in the spectral range from 10 to 16 nm. It is assumed that a plasma is produced due to the interaction of an ultrashort laser pulse with a beam of clusters, dust or nanotubes of one of the eight elements from Er to Re. Laser action in such experiments can appear at two transitions: at the $4d^9 5d\,[J=0] - 4d^9 5p\,[J=1]$ transition, for which the population inversion mechanism is similar to the mechanism existing at the 0–1 transition in Ne- and Ni-like ions; and at the $4d^9 5f\,[J=1] - 4d^9 5d\,[J=1]$ transition, for which the population inversion is produced due to the reabsorption of photons. Optimal conditions are determined for achieving the most efficient short-wavelength lasing for the specified geometry of a plasma filament of a homogeneous density. It is shown that the conversion efficiency of the pump pulse energy to the soft X-ray energy in the range from 10 to 16 nm exceeds 10 % for all the ions studied.**

Keywords: *simulation of X-ray lasers, atomic kinetic calculation.*

1. Introduction

During the last twenty-five years after the advent of the first X-ray lasers, the active medium of these lasers was a plasma produced upon the interaction of pump laser radiation with a solid (foil) [1–5]. The first X-ray lasing experiments were performed by using Ne-like ions [1, 3]. Later studies showed that the scheme with Ni-like ions is more efficient because Ni-like ions (emitting at the same wavelength as Ne-ions) can be produced at electron temperatures lower by several times. In addition, the optimal electron density in the case of Ni-like ions and, hence, recombination radiation losses in a plasma are considerably smaller than in the case of Ne-like ions [5] (see reviews [2–4]).

During the past decade, progress has been achieved in the solution of main problems in the development of X-ray lasers such as (i) the reduction of a laser size, (ii) increase in the pump pulse energy, (iii) increase in a pulse repetition rate, (iv) modification of the properties of a target surface for increasing the pump pulse energy input, (v) improvement of the plasma homogeneity for decreasing the divergence of the output short-wavelength radiation and increasing its coherence, (vi) increasing the radiation intensity homogeneity in the focal spot, etc. One of the most important problems is the optimisation of parameters of a laser emitting in the range 10–16 nm, for which multilayer mirrors with the high reflectance have been developed [6, 7].

The conversion efficiency of the pump pulse energy to a short-wavelength radiation pulse in modern X-ray lasers is $\eta \sim 10^{-6} - 10^{-5}$. The maximum output energy of laboratory X-ray lasers achieves 20–30 μJ [7]. At present these lasers are used in biology, medicine, and physics.

The low conversion efficiency is caused by the following reasons: (i) a weak absorption of the pump laser radiation in a target due to its reflection and scattering; (ii) a small volume of the active medium: a solid target is expanded during and after irradiation by a pump pulse, and favourable conditions for lasing are achieved in a 40–50-μm-thick plasma layer; and (iii) a short lifetime of the population inversion (a few tens of picoseconds).

The optimal electron density for amplifying spontaneous emission at 10–16 nm in Ne-like ions is $n_e^{opt} \approx 10^{21}$–$10^{22}$ cm^{-3} and the electron temperature is $T_e \geqslant 1.5$ keV. In the case of Ni-like ions, $n_e^{opt} > 10^{20}$ cm^{-3} and $T_e > 0.5$ keV. For such densities, in both cases the radiative losses in the plasma due to recombination emission and bremsstrahlung are so high that the optimal state of the plasma cannot be maintained in modern laboratory setups. Amplification is usually observed by using rather short (no longer than 1 ps) pump pulses. In this case, rather high values of T_e are achieved, so that amplification occurs in the ionisation regime: the optimal degree of ionisation of an ion increases by unity for a few tens of picoseconds.

In this connection the search for more efficient X-ray lasers providing the higher gains (compared to Ne- and Ni-like ions) at the lower values of T_e and n_e is of current interest. An X-ray laser based on Pd-like ions belongs to such lasers. Another, no less urgent problem, is the study of different pumping schemes providing considerably higher absorption of the pump radiation in the plasma.

The first observations of the amplified spontaneous emission at the $4d^9 5d[J=0] - 4d^9 5p[J=1]$ transition at 41.8 nm in the Pd-like XeIX ions [8, 9] showed that this X-ray laser had a considerably higher gain and was more efficient than X-ray laser based on Ne- and Ni-like ions. This is explained by at least two reasons:

E.P. Ivanova Institute of Spectroscopy, Russian Academy of Sciences, 142190 Troitsk, Moscow region, Russia;
e-mail: eivanova@isan.troitsk.ru

Received 12 July 2007; revision received 9 January 2008
Kvantovaya Elektronika **38** (10) 917–922 (2008)
Translated by M.N. Sapozhnikov

(i) The ionisation of electron shells with the principal quantum number $n = 6,\ 7$ occurs at comparatively low values of T_e due to relatively large ionisation cross sections.

(ii) The optimal electron density is relatively low: $n_e^{opt} \sim 3 \times 10^{18} - 5 \times 10^{19}$ cm^{-3} for Pd-like ions with the atomic number $Z = 54 - 75$, respectively. Therefore, recombination radiation and bremsstrahlung losses in the X-ray laser based on Pd-like ions are considerably lower.

In [8, 9], a plasma was produced upon ionisation of xenon gas in a capillary tube by a high-intensity ultrashort pump laser pulse. Although the pump parameters and gas pressure in tubes were quite close in both experiments [8] and [9], the results obtained in these papers were considerably different. Thus, the output radiation intensity observed in [8] was not saturated in the plasma of length $L \approx 10$ mm, whereas in experiments [9] the saturation was achieved for $L = 4$ mm. We interpreted experimental results [8, 9] in our previous paper [10]. We determined plasma parameters T_e and n_e achieved in these experiments and proposed a number of refinements of the pump scheme and changes in the target parameters. This should result in a considerable increase in the quantum yield of X-rays.

Paper [11] published in 1994 initiated the investigations of plasmas produced in the interaction of intense laser radiation with a beam of atomic clusters. It was shown in many experiments of various authors that the interaction of an intense laser pulse with a cluster target can lead to the formation of the plasma whose temperature exceeds by a few orders of magnitude the temperature of the plasma produced by irradiating a gas or a solid target by the same pulse. The main reason is that the pump radiation was almost completely absorbed in such plasma.

The idea of obtaining X-ray lasing in the plasma produced by irradiating a beam of xenon clusters by laser pulses was discussed in our paper [12]. This approach was first realised in experiments [13] where a strongly nonlinear dependence of the 41.8-nm radiation intensity of XeIX ions on the concentration of xenon atoms was observed. The optimal plasma density determined in [13] was consistent with experimental results obtained in [8, 9] and our calculations [10].

Lasing at 10–16 nm can be obtained on transitions of heavy Pd-like ions with the nuclear charge $Z > 67$. During the last decade, the spectra of Pd-like ions with $Z = 52 - 60$ have been experimentally investigated in detail ([14] and references therein). The identification of the wavelengths of transitions between the excited states of the Pd-like ion with $Z > 60$ by the known experimental methods is strongly complicated due to a high intensity of the background spectrum of recombination radiation and bremsstrahlung. Spectroscopic data for heavy Pd-like ions ($64 < Z < 83$) are known from the only paper [15]. In [15], only the two most intense $3d^{10}[J = 0] - 3d^9 4f[J = 1]$ transitions were observed experimentally. This information is not sufficient for the reproduction of the entire set of energy levels in the Pd-like ion by using standard programs for calculating atomic spectra.

The spectra of heavy Pd-like ions were calculated in our recent papers [16, 17] by the method of relativistic perturbation theory with the model potential in the zero-order approximation. In [16, 17], the energy levels of Ag-, Rh-, and Pd-like ions with $Z \leqslant 86$ were calculated.

At present rather simple technologies are being developed for manufacturing nanoobjects with controllable dimensions such as nanowires, clusters, etc. For example, a standard method for fabrication of a bundle of tin and lead nanowires was presented in [18]. The production of nanowires made of other heavy elements is also being developed. A new direction – the spectroscopy of dust plasma is progressing extensively. In this connection the investigation of the emission of plasma produced in the interaction of an intense laser pulse with a beam of heavy element clusters seems promising.

In this paper, the possibility of the development of X-ray lasers is studied theoretically by assuming that plasma is produced in the interaction of a pump laser beam with a beam of clusters of elements from Er to Re. The plasma parameters optimal for observation of amplified spontaneous emission in Pd-like ions from ErXXIII to ReXXX are found. The rate constants of processes, the level populations of Pd-like ions in plasma, and the gains at transitions in Pd-like ions from ErXXII to ReXXX were calculated by using results obtained in [17]. The method for calculating the rates of processes and the gains is described in [19] and references therein.

2. X-ray laser on transitions of Pd-like ions

Figure 1 shows the two main laser transitions in a Pd-like ion:

(i) $4d_{3/2}5d_{3/2}[J = 0] - 4d_{3/2}5p_{1/2}[J = 1]$ [(5d–5p (0–1)] transition. Amplified spontaneous emission at this transition was observed in [8, 9]. There also exist two other laser transitions from the upper $[J = 0]$ state to the lower $4d_{3/2}5p_{3/2}[J = 1]$, $4d_{5/2}5p_{3/2}[J = 1]$ states. However, the rates of radiative transitions to these states in Pd-like ions with a small enough nuclear charge Z (in particular, in XeIX) are considerably lower, and for this reason they were not observed in [8, 9].

(ii) $4d_{3/2}5f_{5/2}[J = 1] - 4d_{3/2}5d_{3/2}[J = 1]$ [(5f–5d (1–1)] transition. Amplified spontaneous emission at this transition is caused by the reabsorption of photons at the wavelength coinciding with the transition wavelength. The amplification of this type is called 'optical self-pumping' in the literature. There also exist other transitions with the similar amplification mechanism, for example, the $4d_{5/2}5f_{5/2}[J = 1]$–

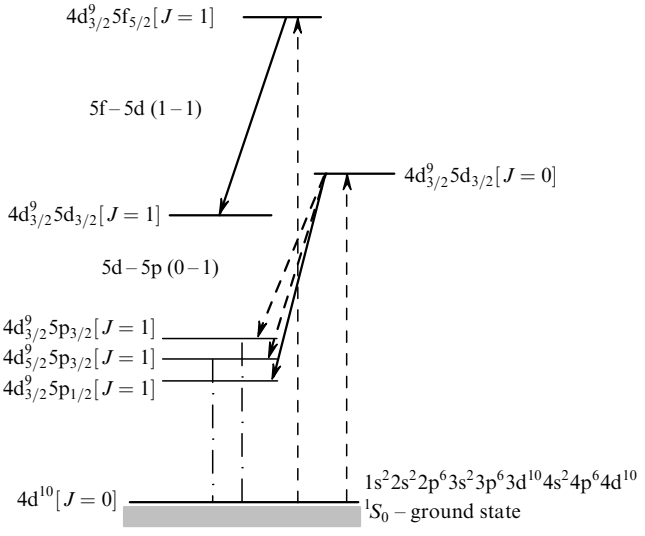

Figure 1. Laser transitions in Pd-like ions.

$4d_{5/2}5d_{3/2}[J=1]$ transition. Note that amplification at 'optically self-pumped' transitions can occur in the sufficiently dense plasma.

Figure 2 shows the wavelengths of three laser transitions in Pd-like ions with $Z = 67 - 78$. In [8, 9], amplification at transitions of the second type was not observed. In ions with a relatively small Z, the gain caused by reabsorption of photons is relatively small. However, the optimal density of plasma increases with increasing Z and, therefore, amplification at transitions of the second type increases. This was shown earlier for Ne- and Ni-like ions [20].

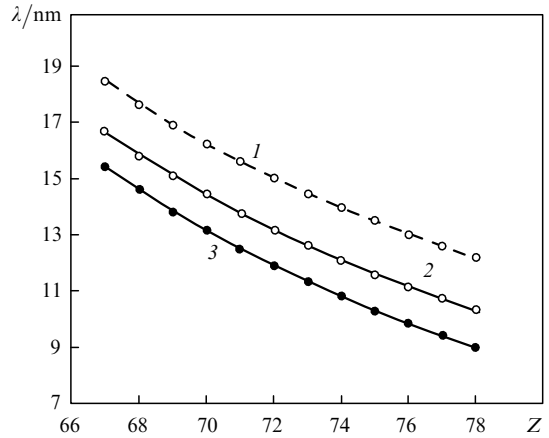

Figure 2. Dependences of wavelengths of the $4d_{3/2}5f_{5/2}[J=1]-4d_{3/2}5d_{3/2}[J=1]$ (*1*), $4d_{3/2}5d_{3/2}[J=0]-4d_{5/2}5p_{3/2}[J=1]$ (*2*) and $4d_{3/2}5d_{3/2}[J=0]-4d_{3/2}5p_{1/2}[J=1]$ (*3*) laser transitions in Pd-like ions on the atomic number.

In this paper, the level population kinetics for Pd-like ions from ErXXIII to ReXXX was calculated assuming that:

(i) Plasma has the form of a cylinder of diameter $d = 100$ μm and length L.

(ii) Parameters of an ultrashort pump pulse provide the instant plasma production during the action of the pump pulse on a beam of clusters (nanowires or dust).

(iii) The electron temperature T_e and electron density n_e of plasma remain constant. Radiative losses due to emission of ions and recombination radiation and bremsstrahlung for plasma densities under study in the time interval $\tau < 20$ ps are negligible. The expansion of plasma with $d = 100$ μm during this time interval is insignificant.

(iv) For $\tau = 0$, all ions in plasma are in the ground state of the Pd-like ion.

(v) Ionisation of Pd-like ions is taken into account.

(vi) The energy distributions of electrons and ions are Maxwell (it is found that the shape of the velocity distribution of electrons is not important in our calculation).

(vii) The ion temperature is $T_i = T_e/10$.

The time-dependent gains $g(n_e, T_e, d|\tau)$ were calculated for each ion from ErXXIII to ReXXX for a set of values of T_e and n_e. The optimal value $n_e = n_e^{opt}$ was determined for each transition for the specified T_e from the condition that the time-averaged value of $\hat{g}(n_e^{opt}, T_e, d|\tau)$ has the maximum value. The time interval for averaging was chosen by considering the time dependences $g(n_e, T_e, d|\tau)$. Figure 3 shows the time dependences for the 13.15-nm 5d – 5p (0 – 1) and 16.24-nm 5f – 5d (1 – 1) laser transitions in YbXXV. Calculations were preformed for each transition for three values of T_e, the values of n_e were taken close to optimal ones. Note that the value of n_e^{opt} for the 5d – 5p (0 – 1) transition is approximately smaller by 4.5 times than n_e^{opt} for the 5f – 5p (1 – 1) transition. The decay of the gain for the 5d – 5p (0 – 1) transition (Fig. 3a) is mainly caused by ionisation of YbXXV to YbXXVI, whereas the decay at the 5f – 5d (1 – 1) transition occurs due to collision mixing of the levels resulting in a decrease (disappearance) of inversion. It follows from Figs 3a, b that the time interval of the gain for the 5f – 5d (1 – 1) transition is considerably shorter than that for the 5d – 5p (0 – 1) transition.

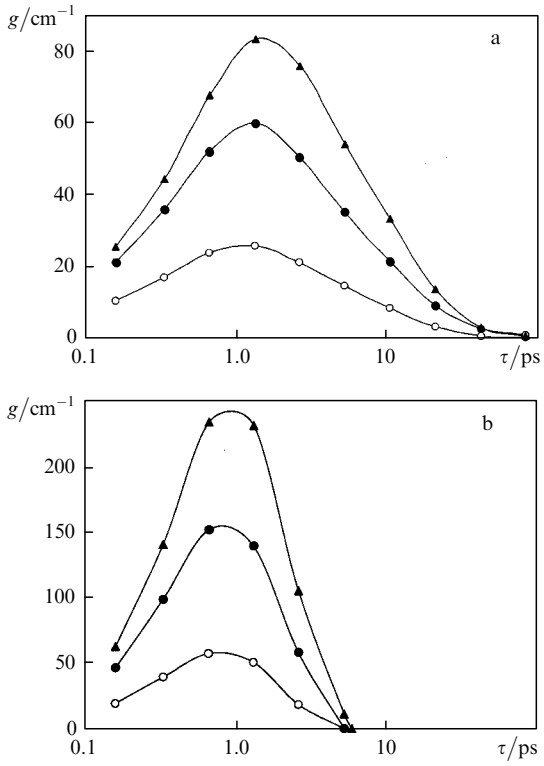

Figure 3. Time dependences of the gain at two transitions in YbXXV for $T_e = 250$ (○), 500 (●) and 1000 eV (▲): the 13.15-nm 5d – 5p (0 – 1) transition [$n_e = 2.2 \times 10^{20}$ cm^{-3}, (a)] and the 16.24-nm 5f – 5d (1 – 1) transition [$n_e = 2.2 \times 10^{20}$ cm^{-3}, (b)].

Figure 4 shows the emission spectra of YbXXV calculated taking into account amplification by using the time-averaged values of $\hat{g}(n_e, T_e, d|\tau)$ for $T_e = 500$ eV. The value of n_e was set equal to n_e^{opt} for each of the transitions. The length of a plasma filament was chosen from the condition of short-wavelength radiation intensity saturation $\hat{g}L_{sat} \approx 14 - 16$. For transitions of the first type in Fig. 4a, the optimal length is $L_{sat} \approx 0.6$ cm, while for transitions of the second type in Fig. 4b, $L_{sat} \approx 0.2$ cm. Figure 4a exhibits the second intense peak at 14.41 nm corresponding to another $4d_{3/2}5d_{3/2}[J=0] - 4d_{5/2}5p_{3/2}[J=1]$ transition of the first type. Apart from the main 16.24-nm 5f – 5d (1 – 1) transition of the second type, Fig. 4b demonstrates other intense lines in the region from 16.3 to 16.8 nm, which correspond to transitions of the second type. One of them is the 16.34-nm $4d_{5/2}5f_{5/2}[J=1] - 4d_{5/2}5d_{3/2}[J=1]$ transition.

For comparatively low T_e (no more than 700 eV), the saturation of the output radiation intensity is determined by

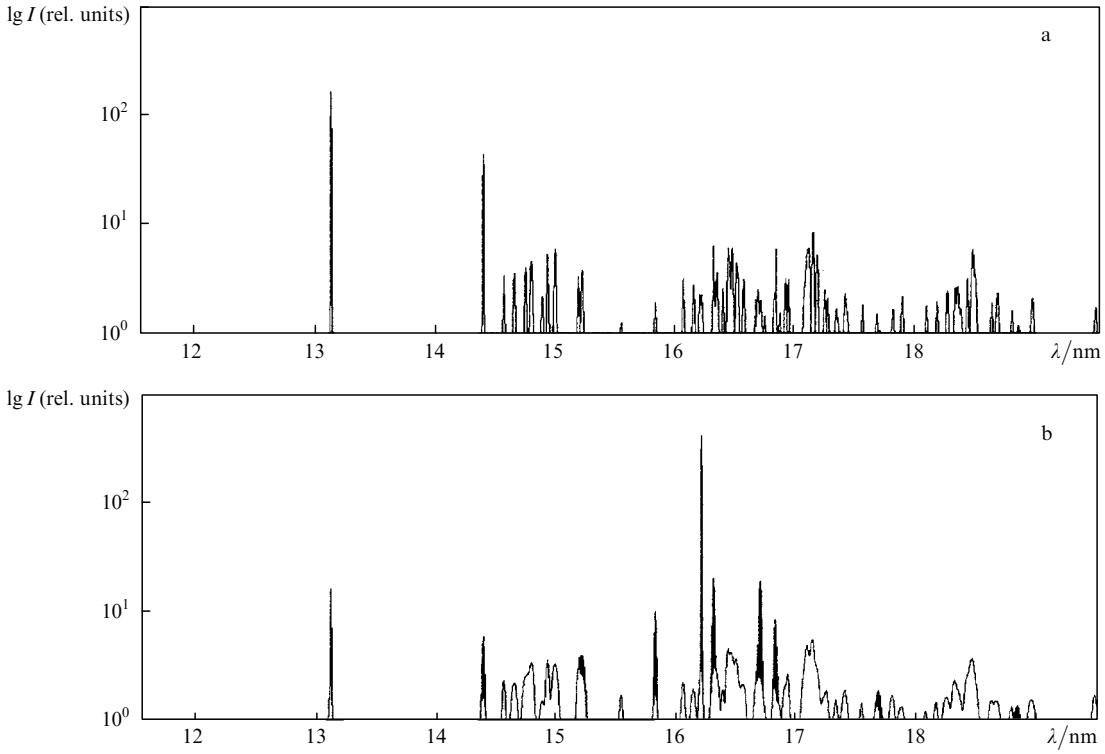

Figure 4. Spectra of YbXXV calculated for $T_e = 500$ eV and $d = 100$ μm taking amplification into account for $n_e = 5 \times 10^{19}$ cm^{-3}, $L = 0.6$ cm (a) and $n_e = 2.2 \times 10^{20}$ cm^{-3}, $L = 0.2$ cm (b).

the time interval of amplification. For large values of T_e (no less than 1000 eV), the time-averaged values of $\hat{g}$ can exceed 1000 cm^{-1}; in this case, the exact value of L_{sat} should be determined from calculations taking into account the interaction between the optical field of short-wavelength radiation and Pd-like ions.

Table 1 presents spectroscopic parameters and gains calculated for transitions of two types in ions from ErXXIII to ReXXX. The wavelengths λ, probabilities of radiative transitions (A_{ij}) and transitions caused by collisions with electrons (R) were calculated by the method of relativistic perturbation theory with the model potential in the zero-

Table 1. Parameters of X-ray lasers on the 5d – 5p (0 – 1) transition and on the 5f – 5d (1 – 1) transition with inversion caused by reabsorption of photons in Pd-like ions from ErXXIII to ReXXX.

Transition	Parameter	Z							
		68	69	70	71	72	73	74	75
5d – 5p (0 – 1)	λ/nm	14.61	13.84	13.15	12.49	11.88	11.32	10.78	10.29
	$A_{ul}/10^{10}$s^{-1}	4.70	5.52	6.44	7.45	8.57	9.80	11.2	12.7
	$A_{l0}/10^{11}$ s^{-1}	2.69	3.30	3.94	4.65	5.44	6.31	7.26	8.29
	$n_e^{opt}/10^{19}$cm^{-3}	3.0	3.0	4.0	4.0	5.0	5.0	6.0	6.0
	$R/10^{10}$ cm^{-3} s^{-1}	9.04	7.90	7.15	6.16	5.64	5.07	4.64	4.04
	$\Delta\nu/10^{12}$ c^{-1}	1.3	1.2	1.7	1.8	1.6	1.8	2.0	2.3
	$I_0/10^{29}$ eV cm^{-3} s^{-1}	0.6	0.6	0.8	0.8	1.0	1.2	1.3	1.4
	$\hat{g}$/cm^{-1}	23.5	21.9	27.8	12.1	29.0	22.7	28.1	14.3
5f – 5d (1 – 1)	λ/nm	17.64	16.92	16.24	15.61	15.02	14.47	13.95	13.47
	$A_{ul}/10^{10}$s^{-1}	7.41	7.92	8.43	8.96	9.50	1.00	1.06	1.12
	$A_{u0}/10^{12}$ s^{-1}	1.06	1.33	1.64	2.00	2.39	2.83	3.31	3.85
	$n_e^{opt}/10^{20}$cm^{-3}	1.3	1.5	1.7	2.1	2.2	2.7	3.1	3.4
	$R/10^{11}$ cm^{-3} s^{-1}	2.43	2.35	2.28	2.19	2.09	2.03	2.00	1.73
	$\Delta\nu/10^{12}$s^{-1}	2.3	2.7	2.8	4.0	3.3	4.4	4.0	4.5
	I_0 (10^{29} eV cm^{-3} s^{-1}	3.3	3.2	3.3	3.5	4.4	4.2	4.5	4.0
	$\hat{g}$/cm^{-1}	122.4	75.25	70.0	44.3	67.8	60.2	71.7	36.4

Note: A_{ul} is the probability of the radiative transition from the upper working level to the lower working level; A_{10} is probability of the radiative transition from the lower $4d_{3/2}5p_{1/2}$ [$J = 1$] working level to the ground state; A_{u0} is the probability of the radiative transition from the upper $4d_{3/2}5f_{5/2}$ [$J = 1$] working level to the ground state; R is the rate of level excitation by electron impact from the ground state; $\Delta\nu$ is the Voigt width of the level; I_0 is the time-averaged radiation capacity of the plasma unit volume at a wavelength of λ (by neglecting amplification); $\Delta\nu$, I_0 and $\hat{g}$ are calculated for $n_e = n_e^{opt}$, $T_e = 500$ eV, and $d = 100$ μm.

order approximation [16, 17]. The Voigt linewidth $\Delta\nu$, radiation capacity I_0 of the unit volume, and gain were calculated for all ions for $T_e = 500$ eV and $d = 100$ μm. The functions $g(\tau)$, $I_0(\tau)$, and $\Delta\nu(\tau)$ for the 5d–5p (0–1) transition in Table 1 were averaged over the time interval from 0 to 20 ps, and for the 5f–5d (1–1) transition – over the time interval from 0 to 5 ps. One can see from Table 1 that all parameters continuously change with changing Z. However, the gain $\hat{g}$ exhibits jumpwise variations depending on Z, which demonstrates a strong sensitivity of inversion to mixing of level populations caused by ion–electron collisions.

Figure 5 shows the dependences of time-averaged gains $\hat{g}$ on n_e for all ions from ErXXIII to ReXXX for $T_e =$ 500 eV. One can see that the gain has large values in a broad density range.

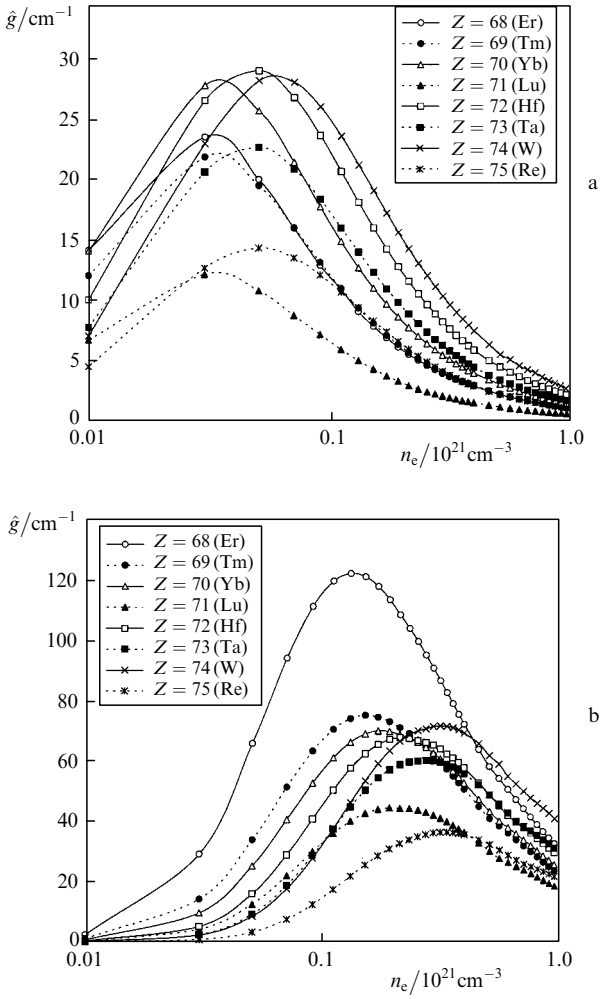

Figure 5. Dependences of the time-averaged gain $\hat{g}$ on the electron concentration n_e for the 5d–5p (0–1) transition averaged from 0 to 20 ps (a) and the 5f–5d (1–1) transition averaged from 0 to 5 ps (b); $T_e = 500$ eV.

3. Conclusions

Our study has shown that for $T_e \approx 500$ eV, $d \approx 100$ μm, and optimal values of n_e for the 5d–5p (0–1) transition, the value of $\hat{g}L$ is $\sim 12 - 15$ for $L = 0.6 - 0.7$ cm. The same values of $\hat{g}L$ for the 5f–5d (1–1) transition are possible for $L = 0.2$ cm.

The gain decay time τ_{las} for each ion decreases with increasing n_e: $\tau_{las} = 30 - 60$ ps for the 5d–5p (0–1) transition and 6–10 ps for the 5f–5d (1–1) transition. The value of n_e^{opt} for the transition of the first type is 4–5 times smaller than that for the transition of the second type. Amplification at the second-type transition can be achieved only by using sufficiently intense picosecond pump pulses. Amplification at the 5d–5p (1–0) transition can be obtained by using pump laser pulses of any duration, the sufficient condition being $T_e \geqslant 250$ eV.

The scheme of an X-ray laser on transitions of Pd-like ions with $Z = 68 - 75$ is undoubtedly the most promising among all the monochromatic low-divergence X-ray sources. The most intense lasing can be obtained in YbXXV, HfXXVII, and WXXIX ions. Laser action in LuXXVI and ReXXX ions is considerably weaker.

The conversion of the pump pulse energy to the X-ray energy in ions considered in the paper can achieve 10 % and more if the pump pulse energy is almost completely absorbed and plasma is homogeneous. In this case, the energy spent for plasma production is several times lower than in X-ray lasers on transitions of Ne- or Ni-like ions emitting at the same wavelength. This is caused first of all by a small electron binding energy of the shell with $n = 6$. Of course, the most important factor is the rate of electron-impact excitation of the upper working level and the depletion rate of the lower working level. If the population inversion exists long enough, the population kinetics of levels taking into account transitions between all the levels plays an important role.

An important advantage of the X-ray laser based on Pd-like ions is a relatively low electron density under conditions optimal for amplified stimulated emission. Without presenting general expressions for radiative losses $dE/d\nu$ due recombination radiation and bremsstrahlung (see, for example, [21]), note that

$$\frac{dE}{d\nu} \sim n_e n_i Z, \tag{1}$$

where ν is the frequency. The product $n_e^{opt} n_i^{opt}$ required to obtain lasing in Pd-like ions at 10–16 nm is two–three orders of magnitude lower than that for Ni-like ions. Because of a low density, radiative losses due to intrinsic emission of ions are also insignificant. This result shows that optimal conditions in relatively large plasma volume can be maintained during long enough time intervals by using compact laboratory sources.

By using Table 1 and Fig. 5 and taking into account that the average population of the upper working level is 0.01, we can estimate the average output power of monochromatic radiation at 10–16 nm as $10^3 - 10^4$ W upon pumping by 1-J picosecond laser pulses with a pulse repetition rate of $10^4 - 10^5$ Hz. Such an estimate is presented in detail in [12].

Acknowledgements. The author thanks N.A. Zinov'ev for his help in the preparation of figures.

References

1. Rozen M.D., Hagelstein P.L., Matthews D.L., Campbell E.M., Has A.U., Whitten B.L., MacGowan B., Turner R.E., Lee R.W., Charatis G., Busch G.E., Shepard C.L., Rockett P.D. *Phys. Rev. Lett.*, **54**, 106 (1985).

2. MacGowan B.J., Da Silva L.B., Fields D.J., Keane C.J., Koch J.A., London R.A., Matthews D.L., Maxon S., Mrowka S., Osterheld A.L., Scofield J.H., Shimkaveg G., Trebes J.E., Walling R.S. *Phys. Fluids B*, **4**, 2326 (1992).
3. Lewis C.L.S., Keenan R., MacPhee A.G., Moore B., O'Rouke R.M.N., Tallents G.J., Dobosz S., Peshete J., Strati F., Wark J.S., Wolfrum E., Pert G.J., MacCabe S.P., Simms P.A., Allot R., Collier J., Danson C.N., Djaoui A., Neely D. *Proc. SPIE Int. Soc. Opt. Eng.*, **3776**, 292 (1999).
4. Kato Y., Nagashima A., Nagashima K., Kado M., Kawachi T., Tanaka M., Hasegawa N., Sukegawa G., Nanba S., Lu P., Sasaki A. *J. Phys. IV*, **11**, Pr. 2-3, (2001).
5. Klisnick A., Kuba J., Ros D., Smith R., Fourcade P., Jamelot G., Miquel J.-L., Wyart J.-F., Chenais-Popovics C., Keenan R., Topping S.J., Lewis C.L.S., Strati F., Tallents G.J., Neely D., Clarke R., Collier J., MacPhee A.G., Bortolotto F., Nickles P.V., Janulewich K.A. *J. Phys. IV*, **11**, Pr. 211-19 (2001).
6. Sun J.R., Wang Ch., Fang Z.H., Wang W., Xiong J., Wu J., Fu S.Z., Gu Y., Wang S.J., Zhang G.P., Zheng W.D., Huang G.L., Guan F.Y., Xie X.L. *Proc. Conf. X-Ray Laser 2006* (Berlin: Springer, 2007) p. 93, 415.
7. Janulevich K.A., Lucianetti A., Priebe G., Sandler W., Nickless P.V. *Phys. Rev. A,* **68**, 051802(R) (2003).
8. Lemoff B.E., Barty C.P.J., Harris S.E. *Opt. Lett.*, **19**, 569 (1994).
9. Sebban S., Sebban S., Haroutunian R., Balcou Ph., Grillon G., Rousse A., Kazamias S., Marin T., Rousseau J.P., Notebaert L., Pittman M., Chambaret J.P., Antonetti A., Hulin D., Ros D., Klisnick A., Carillon A., Jaegle P., Jamelot G., Wyart J.F. *Phys. Rev. Lett.*, **86**, 3004 (2001).
10. Ivanova E.P., Ivanov A.L. *Kvantovaya Elektron.*, **34**, 1013 (2004) [*Quantum Electron.*, **34**, 1013 (2004)].
11. McPherson A., Thompson B.D., Borisov A.B., Boyer K., Rhodes C.K. *Nature*, **370**, 631 (1994).
12. Ivanova E.P., Ivanov A.L. *Zh. Eksp. Teor. Fiz.*, **100**, 844 (2005).
13. Chu H.-H., Tsai H.-E., Chou M.-C., Yang L.-S., Lin J.-Y., Lee C.-H., Wang J., Chen S.-Y. *Phys. Rev. A*, **71**, 061804 (R) (2005).
14. Churilov S.S., Ryabtsev A.N., Wyart J.-F., Tchang-Brillet W.Ü.L., Joshi J.N. *Phys. Scripta*, **71**, 589 (2005).
15. Sugar J., Kaufman V., Rowan W. *J. Opt. Soc. Am.*, **10**, 799 (1993).
16. Ivanova E.P. *Opt. Spektrosk.*, **94**, 181 (2003).
17. Ivanova E.P. *Opt. Spektrosk.*, **103**, 757 (2007).
18. Michotte S. *Int. J. Mod. Phys. B*, **17**, 4601 (2003).
19. Ivanov L.N., Ivanova E.P., Knight L.V., Molchanov A.G. *Phys. Scripta*, **53**, 653 (1996).
20. Ivanova E.P., Zinoviev N.A. *Phys. Lett. A*, **274**, 239 (2000).
21. Abou-Ali Y., Demir A., Tallent G.F., Edwards M., King R.E., Pert G.J. *J. Phys. B: At. Mol. Opt. Phys.*, **36**, 4097 (2003).